DISEASES AND DISORDERS

A novel mouse model of chronic suppurative otitis media and its use in preclinical antibiotic evaluation

Kelly M. Khomtchouk[1], Ali Kouhi[1,2]*, Anping Xia[1]*, Laurent Adonis Bekale[1], Solange M. Massa[1], Jolien M. Sweere[3], Daniel Pletzer[4,5], Robert E. Hancock[4], Paul L. Bollyky[3], Peter L. Santa Maria[1]†

Copyright © 2020 The Authors, some rights reserved; exclusive licensee American Association for the Advancement of Science. No claim to original U.S. Government Works. Distributed under a Creative Commons Attribution NonCommercial License 4.0 (CC BY-NC).

Chronic suppurative otitis media (CSOM) is a neglected pediatric disease affecting 330 million worldwide for which no new drugs have been introduced for over a decade. We developed a mouse model with utility in preclinical drug evaluation and antimicrobial discovery. Our model used immune-competent mice, tympanic membrane perforation and inoculation with luminescent Pseudomonas aeruginosa that enabled bacterial abundance tracking in real-time for 100 days. The resulting chronic infection exhibited hallmark features of clinical CSOM, including inhibition of tympanic membrane healing and purulent ear discharge. We evaluated the standard care fluoroquinolone ofloxacin and demonstrated that this therapy resulted in a temporary reduction of bacterial burden. These data are consistent with the clinical problem of persistent infection in CSOM and the need for therapeutic outcome measures that assess eradication post-therapeutic endpoint. We conclude that this novel mouse model of CSOM has value in investigating new potential therapies.

INTRODUCTION

Chronic suppurative otitis media (CSOM) affects more than 330 million people worldwide and is the most common cause of permanent hearing loss among children in the developing world (*1*). CSOM is now considered a neglected tropical pediatric disease, and treatment options have not improved in a decade (*2*, *3*). It is characterized by a chronically discharging and infected middle ear, with the bacteria *Pseudomonas aeruginosa* (most common) and *Staphylococcus aureus* accounting for approximately 80% of disease (*4*–*6*). Bacteria colonize the middle ear through a hole in the tympanic membrane and soon thereafter establish a biofilm community, thereby complicating attempts to treat and fully eradicate infection (*7*). Clinicians diagnose CSOM after observing a chronically discharging middle ear and collecting swabs from the middle ear for microbiological culture tests. These have been shown to have a high false-negative rate, often coming up as culture negative despite evidence of infection by electron microscopy or polymerase chain reaction (PCR) (*8*).

P. aeruginosa's adaptive resistance, due to the biofilm growth state and persister cells, a subpopulation of metabolically inactive bacteria within *P. aeruginosa* biofilms, contribute substantially to the difficulties encountered in treating CSOM (*9*, *10*). Fluoroquinolone antibiotics, the current standard of care in clinical CSOM, are effective in killing metabolically active free swimming bacteria but are less effective against biofilms and can enhance the formation of biofilms and induce persister cells (*11*, *12*). Even after aggressive therapy, persister and adaptively resistant cells can repopulate the biofilm niche after fluoroquinolone therapy is discontinued (*13*, *14*). Because there is no effective treatment for these biofilm persister cells, the end result is multiple rounds of surgery to debride the biofilm and a lifelong struggle with this disease. Surgical success rates are as low as 60% (*15*).

One factor that limits the development of new therapies for CSOM is a lack of appropriate animal models to study the disease. The majority of what is known about CSOM is adapted from acute infection models and models that do not involve bacteria typically known to cause CSOM (*16*). In animal models of acute otitis media, there is dose-dependent gross bacterial invasion and widespread cochlear injury or rapid clearance of the pathogen unrepresentative of the human disease (*16*). These represent the limitations of studying a chronic condition in acute infection models. A model recreated in mice is ideal given their anatomical and physiological similarity to the human middle ear, the natural occurrence of otitis media, the large background research defining their genome and immune system, and the ability to generate large and efficient in vivo throughput screens for therapeutics in a consistent, efficient, and reproducible way. Until now, there has not been an animal model of CSOM that replicates human disease in terms of the chronicity of infection, tolerance, and the use of the human pathogen *P. aeruginosa*, as previous mouse models use natural murine pathogens and do not result in suppuration chronic wound (*17*). Larger animals are difficult to study given the tortuosity of their external ear canals, preventing direct middle ear access (*18*). A nonhuman primate model of CSOM was only successful in 10%, and the infection did not last beyond 3 weeks (*18*).

To overcome these gaps in rigor, we propose to investigate in vivo within the validated chronic infection model here. We have developed a novel model that mimics the human infection in comparable microbiology and histopathology and also demonstrates recalcitrance, i.e., recurrence of disease after antibiotic cessation. The model shows reestablishment of active infection after the cessation of topical antibiotic treatment, which can be used as a primary outcome measure for testing novel antimicrobials against CSOM.

RESULTS

Generation of a *P. aeruginosa* CSOM mouse model

We first introduced *P. aeruginosa* into the middle ear space. Luminescent bacteria were directly inoculated into the middle ear through a

[1]Department of Otolaryngology, Head and Neck Surgery, Stanford University, Stanford, CA, USA. [2]Department of Otolaryngology, Head and Neck Surgery, Tehran University of Medical Sciences, Tehran, Iran. [3]Department of Medicine, Infectious Diseases, Stanford University, Stanford, CA, USA. [4]Department of Microbiology and Immunology, University of British Columbia, Vancouver, BC, Canada. [5]Department of Microbiology and Immunology, University of Otago, Dunedin, New Zealand.
*These authors contributed equally to this work.
†Corresponding author. Email: petersantamaria@stanford.edu

Downloaded from http://advances.sciencemag.org/ on September 11, 2020

perforated eardrum, with or without prior Eustachian tube occlusion. The timeline for model development is shown in Fig. 1A. Model development and the anatomy of the middle ear are shown in Fig. 1B. These studies used CBA/CaJ mice due to their conserved hearing over at least 2 years of life, making it optimal to study hearing loss, and the C57Bl/6J strain, a commonly used mouse line for immunological studies (*19*).

We asked how the bacterial inoculum affected the establishment of chronic disease in this model. Dose-escalated inoculation of *P. aeruginosa* PAO1 into the middle ear enabled determination of the dose necessary to achieve chronic infection and subsequent characterization of grades of disease resulting from the infection. The outcome of a chronic infection on the tympanic membrane wound was determined using a scoring key developed to assess middle ear infections. The in vivo grading of chronic middle ear infections was performed by an otologist and was based on the clinical features used to grade and classify diseases in humans, including factors of visible inflammation, presence of tympanic membrane perforation, presence of exudate or suppuration, and inflammatory signs on the middle ear mucosa (images of grading criteria; fig. S1).

Next, the correlation between the transtympanic and transcervical methods in the development of chronic infection was determined by assessing recovered colony-forming units (CFU; fig. S2). The high degree of correlation ($r^2 = 0.875$, $P = 0.002$) indicated that the transtympanic method was a suitable substitution for the transcervical method in the CSOM model, with the former allowing for a minimally invasive procedure that could be done in less than 2 min rather than the invasive surgery and long recovery times required in the transcervical model.

At a bacterial inoculation (1.64×10^7 CFU) of PAO1 that resulted in reproducible chronic infections using the transtympanic method of Eustachian tube occlusion, most of the CBA/CaJ mice demonstrated healing of their tympanic membrane wound (66%, $n = 23/35$ at grade 0, I, or II), with only 34% displaying the hallmark signs of CSOM ($n = 12/35$ at grade III or IV). The inoculation dose for CBA/CaJ mice was then further increased (to 2.4×10^7 CFU) to achieve highly reproducible open wounds (100% of the group, $n = 10/10$ at grade IV) (Fig. 2A, left; table of grading criteria, Fig. 2B).

The use of the lower dose (1.64×10^7 CFU) of strain PAO1 in C57Bl/6J mice with transtympanic Eustachian tube occlusion resulted in less severe middle ear infections relative to CBA/CaJ mice, most of which were associated with complete healing of the preexisting tympanic membrane perforation, a diagnosis consistent with otitis media with effusion (25/32 at grade I, representing effusion collection in the middle ear and observed bulging behind an intact tympanic membrane; Fig. 2A, middle). In C57BL/6J mice, where the

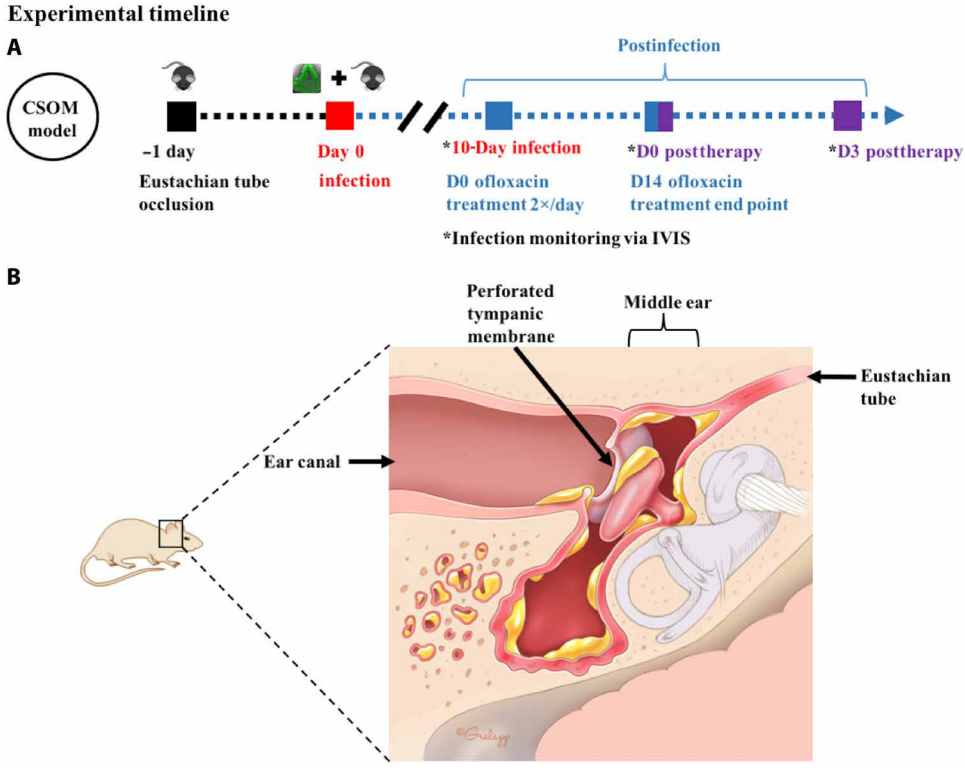

Fig. 1. Generation of a *P. aeruginosa* chronic suppurative otitis media mouse model. Model development scheme. (**A**) Timeline for bacteria inoculation and antibiotic administration. Mice underwent procedures of Eustachian tube occlusion and acute tympanic membrane perforation 1 day before bacteria inoculation. Infection was monitored after inoculation in live anesthetized animals with the LagoX In Vivo Imaging System (IVIS). Antibiotic treatment (two times per day) began at day 10 after infection and continued for 14 days. After treatment, the mice were monitored via IVIS for disease recurrence. (**B**) Axial view of middle ear anatomy relevant to the generation of a mouse model of chronic suppurative otitis media (CSOM; Illustrator: Chris Gralapp). Infection presented in the middle ear space and ear canal. In the image, the tympanic membrane is perforated; in our model, this procedure is performed before bacterial inoculation. Bacterial inoculation and antibiotic administration are able to pass into the middle ear space through the open tympanic membrane via the ear canal. In some instances, blocking the Eustachian tube before bacterial inoculation was used to promote infection. Eustachian tube occlusion was performed via a transtympanic or transcervical procedure with insertion of Gutta Percha points and described further in Materials and Methods.

Downloaded from http://advances.sciencemag.org/ on September 11, 2020

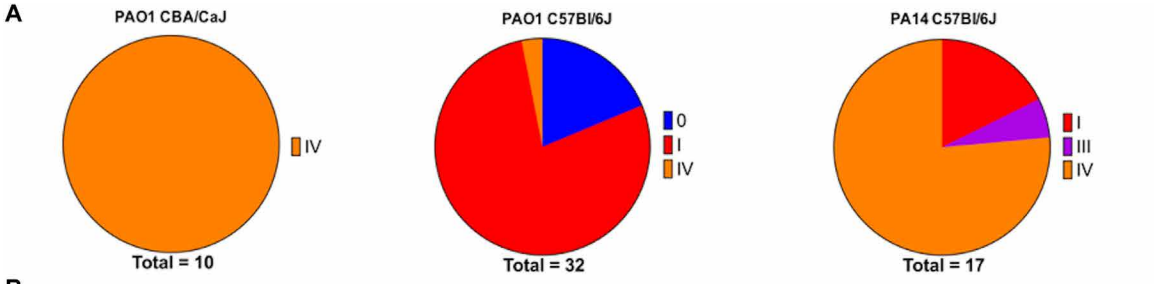

B

	Grade	Clinical features
Chronic infection	0	Tympanic membrane intact with no effusion visible
	I	Tympanic membrane intact with effusion present
	II	Perforation with no effusion visible
CSOM	III	Perforation with suppuration (CSOM)
	IV	CSOM and mucosal disease (thickened and red mucosa)

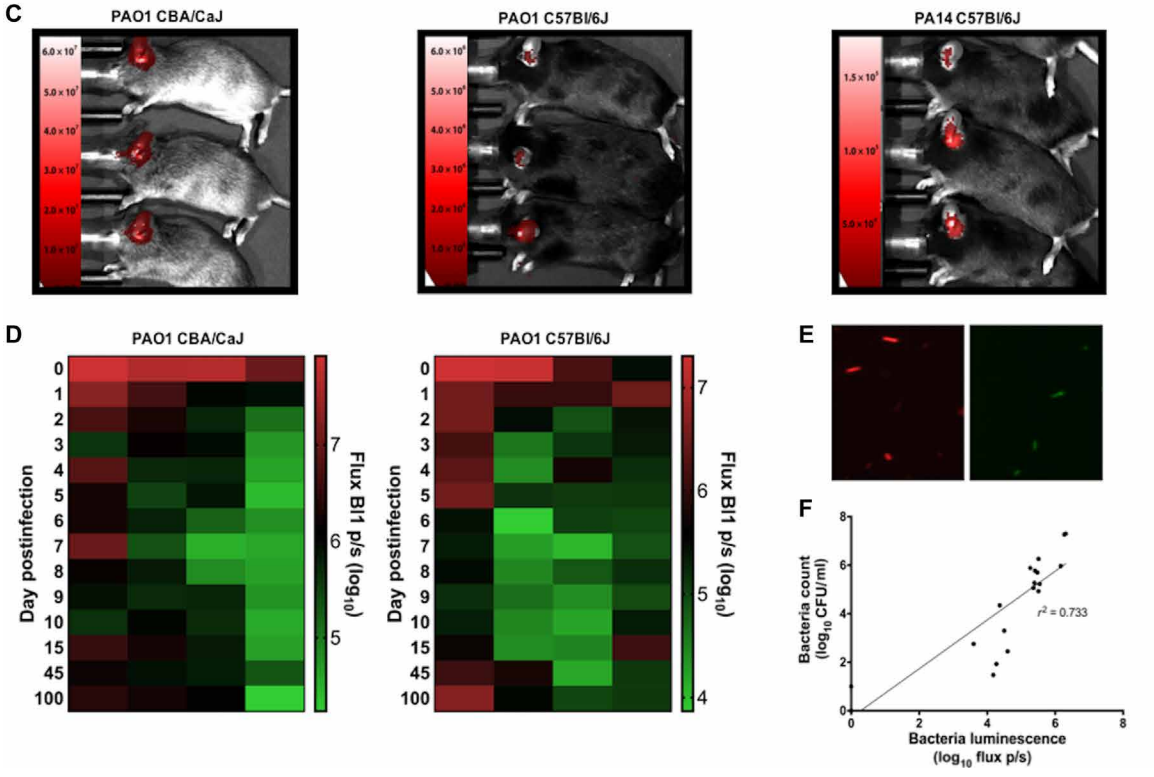

Fig. 2. Characterization of a novel mouse model of *P. aeruginosa* CSOM. (**A**) Infections graded by otologists. The number corresponding to each grade, from left to right: PAO1 CBA/CaJ, PAO1 C57Bl/6J, and PA14 C57Bl/6J. (**B**) Mouse CSOM clinical grading criteria. (**C**) CSOM monitored by IVIS in CBA/CaJ mice [representative images of day 14 postinoculation (dpi)]. Red signal was false-colored luminescence in radiance units at 14 dpi, from left to right: PAO1 CBA/CaJ, PAO1 C57Bl/6J, and PA14 C57Bl/6J. (**D**) Long-term CSOM stability. Time-dependent bacterial bioluminescence of PAO1 CSOM of CBA/CaJ (left) and C57BL/6J (right) mice in a CSOM model ($n = 4$ per group, individual mice in each column). Green indicates reduced and red indicates higher bacterial burden. Chronic infection was still present in all animals shown up to day 100. (**E**) Fluorescent bacteria in middle ear effusion of CBA/CaJ mouse CSOM after 14 dpi. Red fluorescence (PAO1.mCherry) and green fluorescence (pUCP.eGFP). (**F**) Bacterial burden of disease measured with IVIS and conventional CFU/ml at recovery are highly correlative, suggesting IVIS is a useful surrogate for quantitative in vivo estimation of bacteria. Bacterial numbers in vivo measured by luminescent signal of PAO1.lux and reported as background subtracted luminescence intensity ($\log_{10}$ p/s).

chronic middle ear infections developed with 1.64×10^7 CFU of strain PAO1, the tympanic perforation healed in nearly all (~97%) mice (Fig. 2A, middle). Further dose escalation (to 2.4×10^7 CFU) resulted in mice that also failed to develop CSOM ($n = 3$). Inoculation of 1.64×10^7 CFU of PA14, a more virulent but commonly used strain of *P. aeruginosa*, without prior occlusion, resulted in 82% CSOM (14/17 at grades III and IV) and 18% (3/12) of grade I infection (Fig. 2A, right). Thus, the optimal conditions in C57Bl/6J mice

Downloaded from http://advances.sciencemag.org/ on September 11, 2020

were inoculation with 1.64×10^7 CFU PA14, where CSOM (grades III and IV) uniquely developed reproducibly without prior Eustachian tube occlusion through a perforated tympanic membrane (Fig. 2A, right). Figure S3 demonstrates that different mouse strains showed differential susceptibility to *P. aeruginosa* strain PA14. Infection with 2.4×10^7 CFU PA14 into a mouse model of eardrum perforation without Eustachian tube occlusion was tolerated in C57BL/6J but was rapidly lethal in CBA/CaJ mice, with mortality rates as high as 60% in the days following inoculation. At doses of more than 1.64×10^7 CFU of either strain of luminescent bacteria, all mice acquired chronic infections, as confirmed with IVIS (in vivo imaging system) imaging at 14 days after inoculation (Fig. 2C).

Characterization of the novel model of CSOM mimicking human disease

The mouse model was assessed for 3 months, examining changes in bacterial luminescence intensity (bacterial luminescence is dependent on metabolically active and oxygen-consuming bacteria). The biofilm infection was maintained for >100 days with minimal changes in burden as measured by IVIS. Real-time monitoring of bacterial infection by evaluating luminescence using IVIS imaging allowed the assessment of infection stability between the initial and terminal time points (Fig. 2D). This indicated a stable infection in the CSOM model over time for both CBA/CaJ and C57Bl/6J mice.

We then asked whether the murine infection had features of human CSOM, including chronic infection that often returns culture-negative results, and biofilm present in the middle ear mucosa. Our CSOM model was characterized by using fluorescence and scanning electron microscopy (SEM) supplemented with culture standards for assessment of chronic biofilm infections. Using techniques similar to those used to culture bacteria from human CSOM infections, bacteria in the middle ear effusion of murine CSOM were difficult to quantify ex vivo and were repeatedly below the limit of detection for quantitative culture (i.e., undetectable CFU, $n = 10$). However, using fluorescently tagged *Pseudomonas* strains, the presence of bacteria in the middle ear effusion of our model was confirmed ex vivo at 14 days after inoculation via microscopy (Fig. 2E). The quantitative assessment was reproducible when performed in tissue homogenates of the whole infection site, including surrounding tympanic bulla bone and middle ear mucosa. Quantitative bacterial measurements (in CFU per milliliter) from ex vivo middle ear homogenate were highly correlated ($r^2 = 0.733$, $P < 0.0001$) with quantitative bacterial readout by IVIS in luminescence light intensity (photon/s; Fig. 2F).

As early as 1 day after inoculation, biofilm structures were detected in the murine CSOM model by SEM (Fig. 3). Cohousing experiments were performed where infected and naïve mice (with tympanic membrane perforation and transtympanic Eustachian tube occlusion) were present in the same cage to allow for potential transmission. However, infected mice never transmitted infection to naïve animals even after cohousing for ~1 month (undetectable middle ear CFU in animals with Eustachian tube occlusion and tympanic membrane perforation, $n = 5$). We also looked for bacterial dissemination in the CSOM mouse model and found that the infection was confined to the inoculated ear (fig. S4). Only during lethal infections ($n = 2$) were bacteria recovered from other tissues (mean CFU/ml per organ: middle ear, 3.2×10^6; trachea, 1.6×10^5; brain, 1.3×10^3; liver, 1.4×10^3; and nasal swab, 1.4×10^2). This contrasts to nasal swabs from the tolerated chronic CSOM model that were repeatedly below the limit of detection for CFU ($n = 6$). Adverse events, including vestibular symptoms, were uncommon, but in one instance,

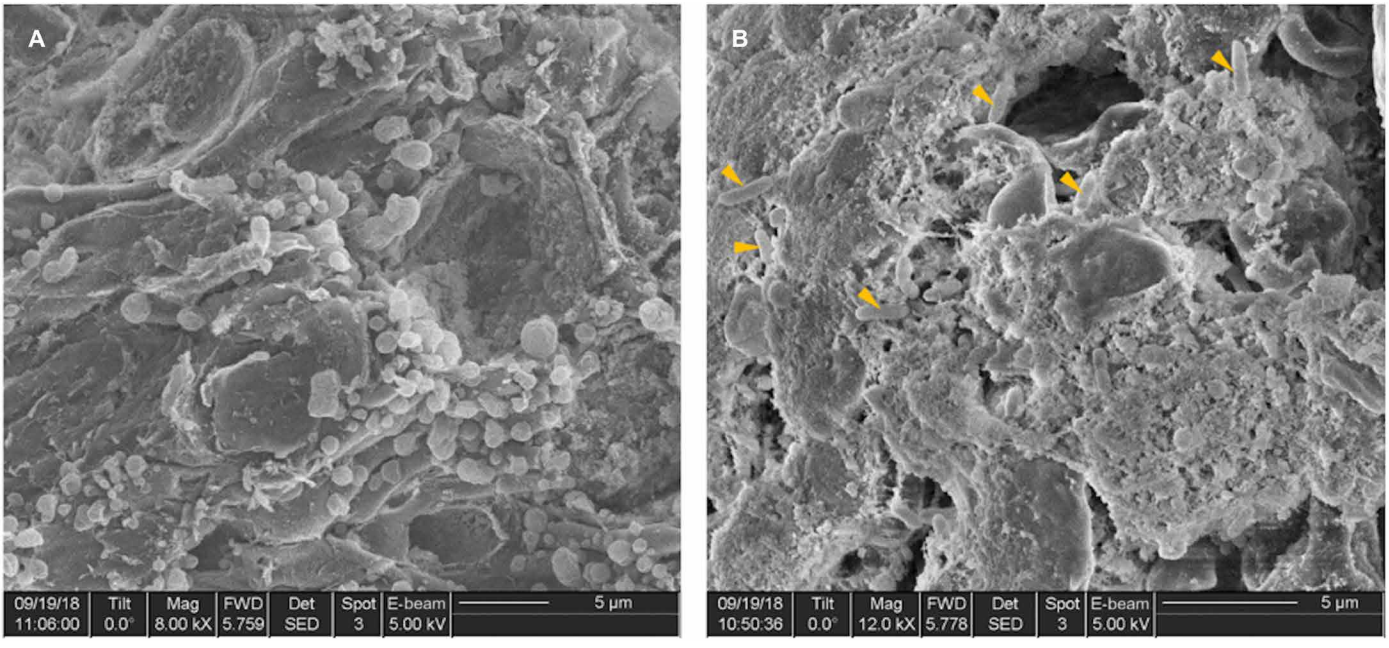

Fig. 3. Demonstration of *P. aeruginosa* mucosal biofilms in a mouse model of CSOM. Scanning electron microscopy (SEM) images of extracted middle ear tissue from (**A**) control (noninfected) middle ear mucosa and (**B**) *P. aeruginosa*–infected middle ear. Small orange arrows indicate *P. aeruginosa* embedded in the mucosal biofilm of the middle ear. C57BL/6J mice were inoculated with *P. aeruginosa* PAO1 1 day following Eustachian tube occlusion and acute tympanic membrane perforation. Biofilm structures were found in vivo on the middle ear mucosal surface within 24 hours after inoculation. Biofilms were not seen in any specimens taken from the noninfected control for which the SEM image demonstrated a normal mucosal surface. This experiment was repeated twice with highly similar results.

Downloaded from http://advances.sciencemag.org/ on September 11, 2020

a *P. aeruginosa* abscess was detected in a CBA/CaJ mouse by IVIS (fig. S5). This animal cleared the middle ear infection but was left with the extraperitoneal abscess.

Recovery-based assays demonstrate the clinical failure of fluoroquinolone therapy

The challenge to validate meaningful in vitro susceptibility testing assays that correspond to outcomes of in vivo antibiotic treatment began with investigating in vitro susceptibility results using assays that examine bacterial growth after recovery (i.e., after therapeutic end point). First, PAO1 was used in the Calgary Biofilm Pin Lib Device for assessing susceptibility via biofilm reduction. We determined the values for the minimum biofilm eradication concentration (MBEC) and the bactericidal biofilm concentration (BBC), respectively (*20*). These results were compared to an in vitro assay of antibiotic tolerance relying on cultures containing late stationary phase bacteria (*21*).

Ten-day-old *P. aeruginosa* PAO1 biofilms were exposed to twofold serial dilutions of ofloxacin. After removal of the antibiotic, 1-day growth recovery was allowed postantibiotic exposure. The fluoroquinolone challenge resulted in a dose-dependent reduction in PAO1 biofilms with an MBEC of 1.5 mg/ml (>1000-fold; the minimum inhibitory concentration of ofloxacin for planktonic cells), the lowest concentration that reduced biofilm growth to below the limit of spectroscopy detection [OD_{650} (optical density at 650 nm) less than 0.1; Fig. 4A]. Where ofloxacin decreased bacterial biofilm to below the limit of detection in the MBEC assay (ofloxacin concentrations of 1.5 and 3 mg/ml), the BBC was then quantified. Bacterial cell growth (an average of 2.7×10^4 CFU/ml) was observed upon recovery of wells challenged with ofloxacin (1.5 mg/ml), revealing a significant reduction ($P < 0.0001$) but still detectable level of biofilm cells after treatment (Fig. 4B). Conversely, 3 mg/ml of ofloxacin eradicated PAO1 cells from the 10-day biofilm culture (undetectable CFU, $P < 0.0001$; Fig. 4B).

Next, we performed the tolerance assay with late stationary phase cultures. A high dose of ofloxacin failed not only to eradicate PAO1 bacteria at the 24-hour recovery time point (an average of 4.3×10^3 CFU/ml), but also, from 24 to 48 hours, there was a progressive increase in CFU per milliliter of surviving bacteria on the same plate (Fig. 4C). PA14 treated with ofloxacin (3 mg/ml) recovered 5.8×10^2 CFU/ml in the tolerance assay.

Recalcitrance in CSOM following fluoroquinolone therapy

Given that there have been no new nor improved drugs developed for CSOM in over the past decade, we wondered whether this mouse model was suitable for assessing therapeutic efficacy for recalcitrant biofilm infection. After the consistency of both the chronic infection and tympanic membrane, perforation status were validated to develop a model of chronic infection and CSOM; it was tested whether treatment with the current standard of care, ofloxacin otic solution (ofloxacin 0.3% Floxin Otic, Daiichi Pharmaceutical Corp., Montvale, NJ, USA), would result in pathogen eradication. After the initial course of ofloxacin treatment, twice daily (BID) for 14 days, in the PAO1 infection models of Eustachian tube occlusion and eardrum perforation, there is a significant decline in posttreatment bacterial quantity (signal under the limit of detection by IVIS, $P = 0.0003$; Fig. 5, A and B). In CBA/CaJ, the IVIS signal averaged 4.698 p/s before treatment. Bacteria are not observable by IVIS after treatment, which indicates that metabolically active bacteria cannot be detected.

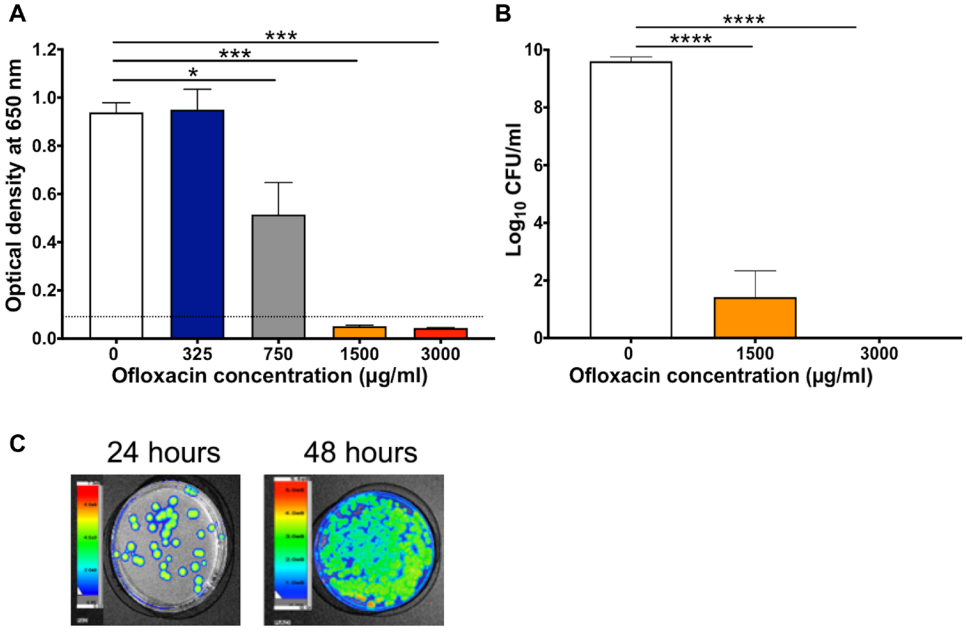

Fig. 4. Susceptibility of *P. aeruginosa* in recovery-based assays. *P. aeruginosa* was tested against ofloxacin in the biofilm-based Calgary Biofilm Device (CBD) assay for the minimum biofilm eradication concentration (MBEC) and biofilm bactericidal concentration (BBC) in a stationary phase assay for tolerance. (**A**) Optical density at recovery phase for MBEC in the CBD biofilm assay. The dashed line indicates the limit of detection by spectrophotometry. (**B**) BBC of ofloxacin against established 10-day-old biofilms of *P. aeruginosa* PAO1 in the CBD biofilm assay. Results are expressed as the number of viable bacteria (in $\log_{10}$ CFU/ml) after 24-hour exposure to ofloxacin. (**C**) Bactericidal activity of ofloxacin in a stationary phase assay for tolerance. PAO1 was treated for 24 hours with ofloxacin (3 mg/ml) before antibiotic removal to examine posttreatment regrowth. Recovery of bioluminescent bacteria was detected after 24 hours and observed to increase through 48 hours. *$P < 0.05$; ***$P < 0.001$; ****$P < 0.0001$

Downloaded from http://advances.sciencemag.org/ on September 11, 2020

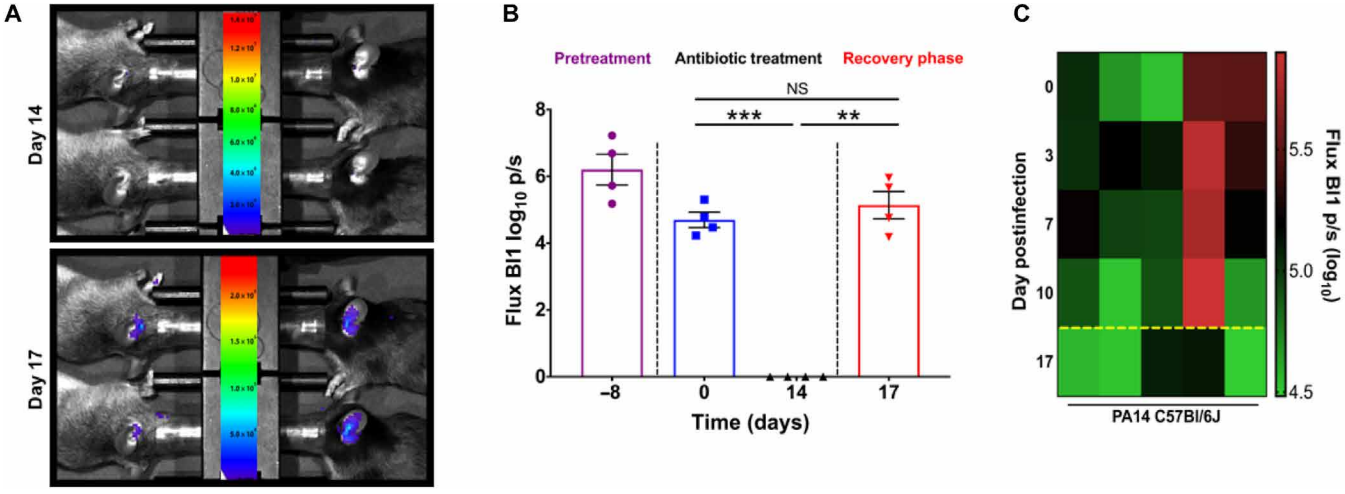

Fig. 5. Recalcitrance in CSOM following fluoroquinolone therapy. *P. aeruginosa* tested against ofloxacin treatment in vivo in mouse CSOM. (**A**) CBA/CaJ and C57Bl/6J mice with Eustachian tube occlusion and tympanic perforation were infected with luminescent PAO1. Ofloxacin was delivered via ear canal twice daily for 2 weeks. Representative IVIS images of mice at final day of treatment (day 14, top) and 3D posttreatment cessation (day 17, bottom) are shown for PAO1 infection in CBA/CaJ and C57Bl/6J mice ($n = 10$ animals per group). Relapse of middle ear infection was observed 3 days after ending topical treatment with ofloxacin (3 mg/ml; representative images are shown). (**B**) Quantitation of IVIS data before, during, and after treatment in CBA/CaJ mice infected with PAO1. IVIS measurements were taken 2 days after bacterial inoculation (day −8), before initiation of ofloxacin treatment (day 0), on the final day of treatment (day 14), and 3 days posttreatment cessation (day 17). $^{**}P < 0.01$; $^{***}P < 0.001$. not significant. (**C**) Time-dependent bacteria luminescence of PA14 during treatment course for chronic middle ear infection in C57BL/6J mice. Bacterial luminescence measurements shown for individual mice (in each column) over time ($n = 5$). Left *y* axis is day of measurement; right *y* axis is background subtracted luminescent intensity ($\log_{10}$ p/s) for the individual mice on recorded day; green indicates reduced and red indicates higher bacterial burden. C57Bl/6J mice were infected with PA14 10 days before beginning treatment. Day 0 is pretreatment measurement corresponding to first day of ofloxacin treatment, delivered via the ear canal twice daily for 2 weeks. Dotted line indicates the end of treatment (day 14). After 14 days of treatment, treatment was stopped. On the third day posttreatment cessation (day 17), IVIS measurements were taken again. PA14 infection response to ofloxacin is markedly different than PAO1 infection response.

By 3 days after treatment cessation, the bacterial burden rebounds, is again measurable by IVIS (in CBA/CaJ, the IVIS signal averaged 5.141 p/s after treatment), and is similar to pretreatment levels (NS; Fig. 5B). The posttreatment end point levels were significantly increased relative to the final day of ofloxacin therapy ($P = 0.0011$). Ofloxacin, 10 μl administered twice daily for 14 days per clinical trial protocol, was overall unsuccessful in eradicating pathogen from any of the animals trialed using the PAO1 infection models in CBA/CaJ and C57Bl/6J mice ($n = 20$). The bactericidal efficacy of ofloxacin against biofilm cells is overestimated by the standard biofilm-based MBEC and BBC assays. The susceptibility of *P. aeruginosa* PAO1 to ofloxacin is most closely mimicked in vitro against stationary phase cultures in a tolerance assay.

The treatment response in the PAO1 CSOM infection models differs from that of the PA14 CSOM, which was detectable over the entire course of ofloxacin treatment (Fig. 5C). Average IVIS posttreatment of PA14 in C57Bl/6J mice was within 5% of pretreatment levels. Figure 5C follows the luminescence by IVIS for five C57Bl/6J mice infected with PA14 in a model of tympanic membrane perforation without Eustachian tube occlusion, followed over time in response to fluoroquinolone therapy.

DISCUSSION

A new model for drug discovery efforts in CSOM

We have validated that our model replicates the human condition of CSOM in bacteriology, using the human biofilm-forming pathogen *P. aeruginosa*, as well as chronicity and recalcitrance to fluoroquinolone therapy. The use of luminescent reporter strains allows for tracking infection in real time and in response to therapy. Our model showed that IVIS has a high correlation with ex vivo bacterial counts, suggesting that our model can be used to document in vivo bacterial quantity and, therefore, track the in vivo response to treatment. As in the clinical setting, our CSOM model often showed "sterile" middle ear effusion cultures, but bacteria are still observed by microscopy and/or grown under aeration. Clinicians currently use a negative culture to indicate disease eradication, and we show why this is inaccurate and why patients experience recurrent disease.

Antibiotics treat exacerbations but may induce chronicity of CSOM

We demonstrated the ability of ofloxacin to successfully eradicate metabolically active *P. aeruginosa* in CSOM, but after cessation of therapy, the bacteria quantity rebounded to pretreatment levels. It is possible that a very small fraction of metabolically active bacteria (below the limit of IVIS detection) repopulates the middle ear; however, in the development of our model, we found that lower doses of *P. aeruginosa* were easily cleared. We propose that it is more likely that small numbers of nonmetabolically active persister cells and adaptively resistant cells, not detected by IVIS, repopulate the middle ear following therapy. This provides an experimental basis for the observed clinical failure of ofloxacin treatment in human CSOM. For chronic bacterial infections, persister cells and the potential induction of adaptive resistance are important barriers for therapeutic development (*22*).

We are now becoming aware that antibiotics not only fail to kill persister cells but also induce the transition of bacteria that are not killed into a persister cell state (*12*, *22*). Sublethal DNA damage in

Downloaded from http://advances.sciencemag.org/ on September 11, 2020

persister cells has been linked to resistance both to the original antibiotic and unrelated antibiotics by enabling resistance genes to be obtained from foreign DNA, using the SOS response–mediated horizontal gene transfer pathway (*11*, *23*). When these persister cells repopulate into metabolically active bacteria, they maintain the same level of sensitivity to antibiotic challenge (*11*, *23*). Unfortunately, this creates a clinical treatment paradox where the only available medical treatment gives a false sense of cure but is likely to contribute to chronicity. Further discouragement is suggested by our finding that fluoroquinolone treatment may worsen infection in CBA/CaJ mice, as the burden trended lower if they were never treated in the first place.

Current standards for therapeutic evaluation in chronic bacterial biofilm disease are inadequate

Many infectious bacterial diseases are biofilm infections, but no antibiofilm drugs have been developed (*24*). Early stages of biofilm formation, including attachment and microcolony formation, were observed within 1 day after inoculation. This is similar to other findings of in vivo biofilm formation within 1 day following *P. aeruginosa* inoculation (*25*, *26*). New drugs aimed at chronic bacterial biofilms involve testing for MBEC and BBC, but these eradication tests are yet to correlate with clinical utility (*20*). We found that in vitro biofilm susceptibility based on these assays did not correlate with in vivo efficacy and, thus, should not form the only basis for predicting preclinical success. Ofloxacin freely diffuses through the biofilm matrix, and impaired diffusion is not the reason for failing to eradicate the biofilm (*21*). Using in vitro tolerance to predict in vivo failure of antibiotic treatments is questionable given that bacterial infection relapse is associated with in vivo drug tolerance (*23*). These biofilm eradication tests are useful as a first pass but do not take into account other factors, including adaptive resistance, persistent bacterial cells, and host chronic inflammation that impair the ability of the immune system to synergize with antibiotics (*24*).

We showed that a lack of in vitro efficacy against stationary phase, but not exponential phase bacteria, was a better predictor of in vivo antibiotic failure. This could be because the mechanisms underlying failure may differ in these two situations. Stationary phase bacteria demonstrate even greater tolerance against many antibiotics than do biofilm, which might reflect increased persister population (*21*). Ofloxacin tolerance in vitro in the stationary phase showed that regrowth of persister cells occurs in phases after ofloxacin treatment ceased, with the number of cells notably increasing from 24 to 48 hours. These reasons justify the in vitro study of persistence for understanding antibiotic failure in vivo. Together, our in vivo model and in vitro tolerance testing are relevant to preclinical therapeutic development for CSOM.

A CSOM model that replicates human disease

Our model has shifted the paradigm for the pathogenesis of CSOM by showing that bacterial strain, state, and dose are key to the development of chronicity. Previously, it was thought that Eustachian tube occlusion and inhibition of tympanic membrane wound healing are necessary precursors to CSOM (*27*, *28*). Eustachian tube dysfunction likely establishes a niche for developing a chronic infection but is not necessary for the development of CSOM. The key to the chronicity of CSOM was the inoculation of the middle ear with the right dose and strain of bacteria. Too low inoculation led to no or inconsistent infections; too high led to early inner ear toxicity and neurological morbidity and mortality. Further, unique bacterial strains were optimal in different mouse lines. While we know CSOM is associated with sensory hearing loss, we do not yet understand how or why (*1*, *29*, *30*). The CBA/CaJ mouse is the current gold standard for investigating mechanisms of sensory hearing loss (*19*). Creating this model within this strain allows therapeutic development aimed at preventing sensory hearing loss in CSOM to proceed.

The foundation is set to test preclinical candidates for CSOM

The limitations of this study include the uncertainty regarding how truly it reflects the human disease situation. Patient-specific disease factors are not accounted for in inbred mice. Future investigations into *P. aeruginosa* phenotypic change to mitigate antibiotic challenge are essential to understand the underlying mechanisms of worsening outcomes for patients with chronic and recurrent biofilm disease. Our ongoing work to characterize chronic infection as it progresses in individual animals may help to identify conserved mechanisms relevant to human disease.

This in vivo platform of chronic and recalcitrant infection will allow for discovery of new therapeutics not only for CSOM but also for other mucosal *P. aeruginosa* biofilm diseases, such as chronic tonsillitis, chronic laryngitis, or sinus infection, as well as respiratory infection in cystic fibrosis, diabetic wound ulcers, and many other chronic biofilm infections (*31*). This CSOM animal model can also be used for screening potential tympanic regenerative therapies (*32*). CSOM is a major health problem worldwide and is the leading cause of permanent hearing loss in the developing world. The CSOM animal models developed here provide the potential for insights relevant to human treatment and allow promising therapeutics to be tested in vivo.

MATERIALS AND METHODS

Animals and ethics approval

All animal procedures were approved by the Institutional Animal Ethics Committee (IACUC) at Stanford University. IACUC guidelines were followed with all animal subjects. Mice (6- to 8-week-old CBA/CaJ and C57Bl/6J male) were purchased from or bred from stock acquired from the Jackson laboratory and housed in the Stanford University animal care facility with ad libitum access to food and water. Euthanasia was performed with carbon dioxide followed by secondary method of cervical dislocation.

Construction of bioluminescent and fluorescent *Pseudomonas* strains

The *P. aeruginosa* bioluminescent strains PAO1.lux and PA14.lux were constructed using a mini-Tn7 insertion system. Briefly, plasmid pUC18T-mini-Tn7T-*lux*-Gm (P1 promoter drives constitutive expression of the *luxCDABE* genes) was coelectroporated with helper plasmid pTNS2 (500 ng each) into PAO1 and PA14, respectively, as described earlier (*33*–*35*). Successful transformants, determined by strong luminescence, were selected on 2xYT gentamicin (50 μg/ml) plates and further verified for correct chromosomal insertion by PCR (*36*, *37*). For fluorescence experiments, the green-labeled PA14 strain, carrying the enhanced green fluorescent protein (eGFP) gene on plasmid pUCP23.eGFP, was used (*38*). Fluorescence was measured at 478-nm excitation and 510-nm emission. To chromosomally tag PAO1 with a fluorescence gene, *mCherry* was amplified from plasmid pMCh-23 (*39*) via primer mCherry fwd-NsiI (ATCATGCATGGTGAGCAAGGGCGAGGA) and mCherry_rev_t0-KpnI

Downloaded from http://advances.sciencemag.org/ on September 11, 2020

(CATGGTACCGGGCCCTGGACTCACAAAGAAAAAACGCCCG GTGTGCAAGACCGAGCGTTCTGAACAACGCCAGGGTTTTCCCAGTCA), whereby the reverse primer had a t0 transcriptional terminator sequence incorporated. Next, the P1 promoter was cut from pUC18T-mini-Tn7T-*lux*-Gm via Bam HI and Pst I and cloned onto pUC18T-mini-Tn7T-Gm (*37*). The amplified *mCherry* gene was digested with Nsi I/Kpn I and cloned into Pst I/Kpn I–digested pUC18T-mini-Tn7T-Gm (Pst I and Nsi I have compatible ends), yielding pUC18T-mini-Tn7T-*mCherry*-Gm. Constructs were verified via fluorescence (excitation/emission, 580/610 nm) with a Synergy H1 plate reader (BioTek Instruments Inc., Winooski, VT, USA) and sent for sequencing. Chromosomal insertion of *mCherry* into PAO1 was performed as described above.

Bacterial preparation

Frozen glycerol stocks were streaked on Luria-Bertani (LB) agar and grown overnight at 37°C. All organisms were then cultured in LB from individual colonies at 37°C, shaking at 200 rpm. Cultures were restreaked on LB plates. An isolated colony from the second sub was picked and grown overnight at 37°C in LB under shaking, aerobic conditions.

Growth was monitored using a spectrophotometer at an optical density of 600 nm (OD_{600}). For stationary cultures, bacteria were grown for >1 day at 37°C and 200 rpm. Exponential cultures were grown to an OD_{600} of 0.5 from stationary phase diluted to OD_{600} = 0.05 or directly from isolated colonies. All cultures were split into 1-ml aliquots and centrifuged at 8000*g* for 7 min. Supernatant was discarded, bacteria were washed three times in 0.9 ml of sterile phosphate-buffered saline (PBS), and resuspended to a final concentration for inoculation. The OD_{600} growth curves of bacteria over time (hours) were used to calculate a standard curve for CFU per milliliter from OD_{600}. At various time points, bacteria were diluted and plated for CFU per milliliter.

In vitro drug susceptibility testing

The MBEC and BBC for *P. aeruginosa* were determined using 96-well plates with biofilm inoculating peg lids (Nunc Immuno TSP Lids, Thermo Fisher Scientific). Plates were inoculated from overnight culture diluted to an OD of 0.1 and grown with no aeration at 37°C. Bacterial growth in 96-well plates in broth was confirmed by OD_{650}. Plate pegs were rinsed in 150 ml of sterile Milli-Q H_2O and then challenged with Mueller-Hinton broth (MHB) alone or with twofold dilutions of ofloxacin from 3 mg/ml. Ofloxacin analytical standard (Sigma-Aldrich, MO, USA) was used for in vitro experiments and was dissolved in LB or MHB. After challenge, the plate was rinsed twice as above and sonicated in a new plate of sterile MHB for 15 min at room temperature to transfer biofilm from pegs to the recovery broth in the wells. Plates were then recovered for 1 day at 37°C. The OD_{650} confirmed biofilm growth in the recovery medium for positive control wells, and the MBEC was defined as the lowest concentration of drug below detection limit for the spectrophotometer (SpectraMax M2e, Molecular Devices, San Jose, CA, USA). The BBC was defined by the lowest concentration of a compound that completely prevented visible cell growth upon plating for CFU per milliliter. For stationary phase culture treatments in tolerance studies, stationary phase bacteria (grown for >1 day) was prepared as for inoculation above. After 24 hours of drug treatment, drug was removed by washing five times in PBS as described and plated for recovery on LB agar.

Transcervical Eustachian tube occlusion

Surgery was performed in mice as previously described (*18*). Briefly, under general anesthesia, a transcervical approach was used to identify the bony Eustachian tube, identified medial to the tympanic bulla. This was opened with cautery, and Gutta Percha (Meta-Biomed Co., Republic of Korea) was used to occlude the Eustachian tube. Mice were recovered for 24 hours before inoculation of the middle ear.

Transtympanic Eustachian tube occlusion

The transtympanic method of Eustachian tube occlusion in mice was performed under general anesthesia [intraperitoneal injection of ketamine (65 mg/kg) and xylazine (5 mg/kg)]. After creating a subtotal perforation using a Rosen needle, the middle ear orifice of the Eustachian tube was identified. Gutta Percha (Meta-Biomed Co., Republic of Korea) was inserted to occlude the Eustachian tube. Mice were inoculated simultaneously as below or recovered for 24 hours before inoculation of the middle ear.

Bacterial inoculation

Under anesthesia of 3% isoflurane, bacteria were inoculated (10 μl) into middle ear bulla through open tympanic membrane wounds, and the mice rested on their ventral side until recovery. Control mice received equal volumes of sterile PBS. For *P. aeruginosa*, reproducible chronic infections were obtained with an inoculum of 1.64×10^7 CFU.

Real-time infection tracking

Disease progression was followed by capturing images with open emission using a LagoX IVIS (Spectral Instruments Imaging, AZ, USA). Using isoflurane, mice were placed on the right lateral position to expose the left ear at progressive days after inoculation. Images were initially acquired at 60-s exposure with medium binning. If no signal was detected, mice were reanalyzed at 300-s exposure with high binning. Luminescence was quantified with Aura software (Spectral Instruments Imaging, AZ USA). Background luminescent signal was subtracted from signal coming from the area around the ear. Chronic infection was designated as the presence of infection 14 days after inoculation. Progression was monitored by IVIS as described, after inoculation and daily for 2 weeks. For the months following inoculation, IVIS monitoring was reduced to weekly.

Fluoroquinolone treatment

Floxin Otic (ofloxacin 0.3% solution, Daiichi Pharmaceutical Corporation, NJ, USA) or vehicle (PBS) was directly inoculated into the middle ear after confirmation of an open tympanic membrane wound on day 10 after bacterial inoculation. For PAO1 infection in C57Bl/6J, the tympanic membrane was reperforated before antibiotic treatment. Antibiotic or vehicle treatment was performed twice daily for 2 weeks, allowing the mouse to lie on the ventral side for 5 min after treatment and then recovered from anesthesia (2 to 3% isoflurane), mimicking the clinical trial design of ofloxacin otic (*40*).

In vivo grading of infection

Wound and infection features of CSOM were characterized as in Fig. 2. A clinical otologist blinded to the infection status of the animal graded the mice after 14 days after inoculation using a surgical microscope (Leica Microsystems M320, Germany). The investigator was blinded to the infection status of the animal to reduce detection bias. A summary of the experimental method and timeline for tympanic membrane perforation, Eustachian tube occlusion, bacterial

Downloaded from http://advances.sciencemag.org/ on September 11, 2020

inoculation, fluoroquinolone treatment, and tracking over time by the LagoX IVIS is shown in Fig. 1.

Bacterial burden assessment

The tympanic bulla and other organs were harvested to determine bacterial quantity. To determine bacteria burden via serial dilution, the tissues were minced in 1 ml of sterile PBS, tissues were left shaking for >2 hours at 4°C, and plated on LB agar for CFU per milliliter. Limit of detection for growth is 10^2 CFU/ml.

Microscopy

Fluorophore expressing *P. aeruginosa* was identified in the middle ear effusion of CBA/CaJ mouse in model of transtympanic Eustachian tube occlusion with eardrum perforation after 14 days of bacterial inoculation by microscopy. The effusion from mice infected in the middle ear with PAO1.mCherry ($n = 3$) and PAO1.eGFP ($n = 3$) was fixed at 4% paraformaldehyde and washed with PBS. They were then placed on the slide and covered by coverslip. The *P. aeruginosa* images were captured on a Zeiss LSM 700 confocal microscope (Carl Zeiss). The excitation of 590 nm and emission of 617 nm were used for PAO1.mCherry; excitation of 499 nm and emission of 519 nm were used for PAO1.pUCP.eGFP. Negative controls ($n = 3$) did not show bacteria in either fluorescent wavelength.

SEM and sample processing

Middle ear samples were fixed in 2% glutaraldehyde/4% formaldehyde in sodium cacodylate buffer (pH 7.3) for 24 hours at room temperature and then stored at 4°C. We added 1% OsO4 followed by sequential ethanol washes of 50, 70, 95, and 100%. To remove the ethanol and dry the sample, hexamethyldisilazane was used and then allowed to air dry. The Critical Point Dryer was used to remove the remaining ethanol. Sample was then attached to a 12-mm stub using double stick, carbon-conductive tape and coated with gold/paladium (Au/Pd) at a 60:40 ratio. Using a FEI Strata 235DB dual-beam SEM, images of *P. aeruginosa*–infected middle ear mucosa were taken. Bacterial cells are marked with orange arrows for easier viewing. The representative SEM images of the mucosal surface show *P. aeruginosa* integrating with the native tissue and inflammatory infiltrate at an E-beam of 5 kV.

Statistical analysis

Statistics were performed using GraphPad Prism 7.0 or 8.0 (GraphPad Software Inc., La Jolla, CA, USA). *P* values were calculated using two-tailed *t* test with Welch's correction or a two-tailed Mann-Whitney test with data considered significant when *P* values were below 0.05 as indicated. Pearson *r* was used for determining correlation.

SUPPLEMENTARY MATERIALS

Supplementary material for this article is available at http://advances.sciencemag.org/cgi/content/full/6/33/eabc1828/DC1

View/request a protocol for this paper from *Bio-protocol*.

REFERENCES AND NOTES

1. S. S. da Costa, L. P. S. Rosito, C. Dornelles, Sensorineural hearing loss in patients with chronic otitis media. *Eur. Arch. Otorhinolaryngol.* **266**, 221–224 (2009).
2. M. G. Li, P. J. Hotez, J. T. Vrabec, D. T. Donovan, Is chronic suppurative otitis media a neglected tropical disease? *PLOS Negl. Trop. Dis.* **9**, e0003485 (2015).
3. World Health Organization, *Chronic Suppurative Otitis Media: Burden of Illness and Management Options* (World Health Organization, Geneve, 2004), pp. 1–83.
4. X. Gu, Y. Keyoumu, L. Long, H. Zhang, Detection of bacterial biofilms in different types of chronic otitis media. *Eur. Arch. Otorhinolaryngol.* **271**, 2877–2883 (2014).
5. I. Akyildiz, G. Take, K. Uygur, Y. Kizil, U. Aydil, Bacterial biofilm formation in the middle-ear mucosa of chronic otitis media patients. *Indian J. Otolaryngol. Head Neck Surg.* **65** (suppl. 3), 557–561 (2013).
6. J. Saunders, M. Murray, A. Alleman, Biofilms in chronic suppurative otitis media and cholesteatoma: Scanning electron microscopy findings. *Am. J. Otolaryngol.* **32**, 32–37 (2011).
7. R. D. Wolcott, G. D. Ehrlich, Biofilms and chronic infections. *JAMA* **299**, 2682–2684 (2008).
8. M. Neeff, K. Biswas, M. Hoggard, M. W. Taylor, R. Douglas, Molecular microbiological profile of chronic suppurative otitis media. *J. Clin. Microbiol.* **54**, 2538–2546 (2016).
9. C. de la Fuente-Núñez, F. Reffuveille, L. Fernández, R. E. W. Hancock, Bacterial biofilm development as a multicellular adaptation: Antibiotic resistance and new therapeutic strategies. *Curr. Opin. Microbiol.* **16**, 580–589 (2013).
10. L. R. Mulcahy, J. L. Burns, S. Lory, K. Lewis, Emergence of *Pseudomonas aeruginosa* strains producing high levels of persister cells in patients with cystic fibrosis. *J. Bacteriol.* **192**, 6191–6199 (2010).
11. T. C. Barrett, W. W. K. Mok, A. M. Murawski, M. P. Brynildsen, Enhanced antibiotic resistance development from fluoroquinolone persisters after a single exposure to antibiotic. *Nat. Commun.* **10**, 1177 (2019).
12. T. Dörr, M. Vulić, K. Lewis, Ciprofloxacin causes persister formation by inducing the TisB toxin in *Escherichia coli*. *PLOS Biol.* **8**, e1000317 (2010).
13. I. Keren, N. Kaldalu, A. Spoering, Y. Wang, K. Lewis, Persister cells and tolerance to antimicrobials. *FEMS Microbiol. Lett.* **230**, 13–18 (2004).
14. E. Sun, E. E. Gill, R. Falsafi, A. Yeung, S. Liu, R. E. W. Hancock, Broad-spectrum adaptive antibiotic resistance associated with *Pseudomonas aeruginosa* mucin-dependent surfing motility. *Antimicrob. Agents Chemother.* **62**, e00848–18 (2018).
15. H. E. Tan, P. L. Santa Maria, R. H. Eikelboom, K. S. Anandacoomaraswamy, M. D. Atlas, Type I tympanoplasty meta-analysis: A single variable analysis. *Otol. Neurotol.* **37**, 838–846 (2016).
16. N. H. Davidoss, Y. K. Varsak, P. L. Santa Maria, Animal models of acute otitis media - A review with practical implications for laboratory research. *Eur. Ann. Otorhinolaryngol. Head Neck Dis.* **135**, 183–190 (2018).
17. K. K. Dewan, D. L. Taylor-Mulneix, L. L. Campos, A. L. Skarlupka, S. M. Wagner, V. E. Ryman, M. C. Gestal, L. Ma, U. Blas-Machado, B. T. Faddis, E. T. Harvill, A model of chronic, transmissible Otitis Media in mice. *PLOS Pathog.* **15**, e1007696 (2019).
18. J. E. Dohar, P. A. Hebda, R. Veeh, M. Awad, J. W. Costerton, J. Hayes, G. D. Ehrlich, Mucosal biofilm formation on middle-ear mucosa in a nonhuman primate model of Chronic Suppurative Otitis Media. *Laryngoscope* **115**, 1469–1472 (2005).
19. H. Liu, G. Li, J. Lu, Y.-G. Gao, L. Song, G.-L. Li, H. Wu, Cellular differences in the cochlea of CBA and B6 mice may underlie their difference in susceptibility to hearing loss. *Front. Cell. Neurosci.* **13**, 60 (2019).
20. S. Mulla, A. Kumar, S. Rajdev, Comparison of MIC with MBEC assay for in vitro antimicrobial susceptibility testing in biofilm forming clinical bacterial isolates. *Adv. Microbiol.* **6**, 73–78 (2016).
21. A. L. Spoering, K. Lewis, Biofilms and planktonic cells of *Pseudomonas aeruginosa* have similar resistance to killing by antimicrobials. *J. Bacteriol.* **183**, 6746–6751 (2001).
22. A. Soares, V. Roussel, M. Pestel-Caron, M. Barreau, F. Caron, E. Bouffartigues, S. Chevalier, M. Etienne, Understanding ciprofloxacin failure in *Pseudomonas aeruginosa* biofilm: Persister cells survive matrix disruption. *Front. Microbiol.* **10**, 2603 (2019).
23. I. Levin-Reisman, I. Ronin, O. Gefen, I. Braniss, N. Shoresh, N. Q. Balaban, Antibiotic tolerance facilitates the evolution of resistance. *Science* **355**, 826–830 (2017).
24. J. L. Del Pozo, Biofilm-related disease. *Expert Rev. Anti Infect. Ther.* **16**, 51–65 (2018).
25. J. A. Schaber, W. J. Triffo, S. J. Suh, J. W. Oliver, M. C. Hastert, J. A. Griswold, M. Auer, A. N. Hamood, K. P. Rumbaugh, *Pseudomonas aeruginosa* forms biofilms in acute infection independent of cell-to-cell signaling. *Infect. Immun.* **75**, 3715–3721 (2007).
26. E. Kanno, S. Toriyabe, L. Zhang, Y. Imai, M. Tachi, Biofilm formation on rat skin wounds by *Pseudomonas aeruginosa* carrying the green fluorescent protein gene. *Exp. Dermatol.* **19**, 154–156 (2010).
27. P. L. Santa Maria, S. Kim, Y. K. Varsak, Y. P. Yang, Heparin binding-epidermal growth factor-like growth factor for the regeneration of chronic tympanic membrane perforations in mice. *Tissue Eng. Part A* **21**, 1483–1494 (2015).
28. Y. K. Varsak, P. L. Santa Maria, Mouse model of experimental Eustachian tube occlusion: A surgical technique. *Acta Otolaryngol.* **136**, 12–17 (2016).
29. M. Sone, Inner ear disturbances related to middle ear inflammation. *Nagoya J. Med. Sci.* **79**, 1–7 (2017).
30. V. Tsuprun, S. Cureoglu, P. A. Schachern, P. Ferrieri, D. E. Briles, M. M. Paparella, S. K. Juhn, Role of pneumococcal proteins in sensorineural hearing loss due to otitis media. *Otol. Neurotol.* **29**, 1056–1060 (2008).
31. D. Lebeaux, J.-M. Ghigo, C. Beloin, Biofilm-related infections: Bridging the gap between clinical management and fundamental aspects of recalcitrance toward antibiotics. *Microbiol. Mol. Biol. Rev.* **78**, 510–543 (2014).

Downloaded from http://advances.sciencemag.org/ on September 11, 2020

32. P. L. Santa Maria, M. D. Atlas, R. Ghassemifar, Chronic tympanic membrane perforation: A better animal model is needed. *Wound Repair Regen.* **15**, 450–458 (2007).
33. F. H. Damron, E. S. McKenney, M. Barbier, G. W. Liechti, H. P. Schweizer, J. B. Goldberg, Construction of mobilizable mini-Tn*7* vectors for bioluminescent detection of Gram-negative bacteria and single-copy promoter lux reporter analysis. *Appl. Environ. Microbiol.* **79**, 4149–4153 (2013).
34. D. Pletzer, Y. Braun, H. Weingart, Swarming motility is modulated by expression of the putative xenosiderophore transporter SppR-SppABCD in *Pseudomonas aeruginosa* PA14. *A.V. Leeuwenhoek* **109**, 737–753 (2016).
35. D. Pletzer, S. C. Mansour, K. Wuerth, N. Rahanjam, R. E. W. Hancock, New mouse model for chronic infections by Gram-negative bacteria enabling the study of anti-infective efficacy and host-microbe interactions. *MBio* **8**, e00140–17 (2017).
36. K.-H. Choi, J. B. Gaynor, K. G. White, C. Lopez, C. M. Bosio, R. R. Karkhoff-Schweizer, H. P. Schweizer, A Tn7-based broad-range bacterial cloning and expression system. *Nat. Methods* **2**, 443–448 (2005).
37. K.-H. Choi, H. P. Schweizer, mini-Tn7 insertion in bacteria with single *att*Tn7 sites: Example *Pseudomonas aeruginosa*. *Nat. Protoc.* **1**, 153–161 (2006).
38. H. Woehlk, M. J. Trimble, S. C. Mansour, D. Pletzer, V. Trouillet, A. Welle, L. Barner, R. E. W. Hancock, C. Barner-Kowollik, K. E. Fairfull-Smith, Controlling biofilm formation with nitroxide functional surfaces. *Polym. Chem.* **10**, 4252–4258 (2019).
39. C. L. Berry, A. K. C. Brassinga, L. J. Donald, W. G. D. Fernando, P. C. Loewen, T. R. de Kievit, Chemical and biological characterization of sclerosin, an antifungal lipopeptide. *Can. J. Microbiol.* **58**, 1027–1034 (2012).
40. A. S. Agro, E. T. Garner, J. W. Wright III, I. Cabelleros de Escobar, B. Villeda, M. Seidlin, Clinical trial of ototopical ofloxacin for treatment of chronic suppurative otitis media. *Clin. Ther.* **20**, 744–759 (1998).

Acknowledgments: We thank T. Doyle of Stanford University SCI3 for supporting IVIS analysis, J. Perrino of Stanford University Cell Science Imaging Facility for SEM preparation, P. Secor of the University of Montana for assistance with bacteria protocols, and C. Gralapp for scientific illustrations. **Funding:** We would like to thank the following funding sources: the Stanford Initiative to Cure Hearing Loss by a generous gift from the Bill and Susan Oberndorf Foundation, the Department of Otolaryngology, Head and Neck Surgery, Stanford University, and Action on Hearing Loss Flexi Grant to P.L.S.M.; the NIH LRP from NCATS to K.M.K.; the Stanford Maternal and Child Health Research Institute and the Stanford SPARK Translational Research Program to P.L.S.M., K.M.K., L.A.B., and A.X.; the Stanford Nano Shared Facilities (SNSF) supported by the NSF under award ECCS-1542152 to S.M.M.; and the Michael Smith Foundation for Health Research, the Canadian Institutes from Health Research grant FDN-154287, the Canada Research Chair, and the UBC Killam Professorship to R.E.H. This work was partially supported by the NIH Division of Loan Repayment from NCATS to K.M.K. (awarded January 2018). **Author contributions:** K.M.K., P.L.B., and P.L.S.M. conceived the study and designed and interpreted the experiments. K.M.K., L.A.B., and P.L.S.M. wrote the manuscript. K.M.K., A.K., A.X., L.A.B., and S.M.M. performed and analyzed the experiments. D.P. created critical tools for this study. D.P. and R.E.H. edited the manuscript. D.P., W.H., J.M.S., R.E.H., and P.L.B. provided critical insights and advice. **Competing interests:** K.M.K., L.A.B., P.L.B., D.P., J.M.S., R.E.H., and P.L.S.M. are inventors on patent applications for novel drugs against *P. aeruginosa* (nos. 15/219,073; 62/027721; 62/027698; 63/024,963; and 62/873,717). The authors declare that they have no other competing interests. **Data and materials availability:** All data needed to evaluate the conclusions in the paper are present in the paper and/or the Supplementary Materials. Additional data related to this paper may be requested from the authors.

Submitted 10 April 2020
Accepted 2 July 2020
Published 14 August 2020
10.1126/sciadv.abc1828

Citation: K. M. Khomtchouk, A. Kouhi, A. Xia, L. A. Bekale, S. M. Massa, J. M. Sweere, D. Pletzer, R. E. Hancock, P. L. Bollyky, P. L. Santa Maria, A novel mouse model of chronic suppurative otitis media and its use in preclinical antibiotic evaluation. *Sci. Adv.* **6**, eabc1828 (2020).

Downloaded from http://advances.sciencemag.org/ on September 11, 2020

Science Advances

A novel mouse model of chronic suppurative otitis media and its use in preclinical antibiotic evaluation

Kelly M. Khomtchouk, Ali Kouhi, Anping Xia, Laurent Adonis Bekale, Solange M. Massa, Jolien M. Sweere, Daniel Pletzer, Robert E. Hancock, Paul L. Bollyky and Peter L. Santa Maria

Sci Adv **6** (33), eabc1828.
DOI: 10.1126/sciadv.abc1828

ARTICLE TOOLS http://advances.sciencemag.org/content/6/33/eabc1828

SUPPLEMENTARY MATERIALS http://advances.sciencemag.org/content/suppl/2020/08/11/6.33.eabc1828.DC1

REFERENCES This article cites 39 articles, 7 of which you can access for free
http://advances.sciencemag.org/content/6/33/eabc1828#BIBL

PERMISSIONS http://www.sciencemag.org/help/reprints-and-permissions

Use of this article is subject to the Terms of Service

Science Advances (ISSN 2375-2548) is published by the American Association for the Advancement of Science, 1200 New York Avenue NW, Washington, DC 20005. The title *Science Advances* is a registered trademark of AAAS.

Copyright © 2020 The Authors, some rights reserved; exclusive licensee American Association for the Advancement of Science. No claim to original U.S. Government Works. Distributed under a Creative Commons Attribution NonCommercial License 4.0 (CC BY-NC).

Downloaded from http://advances.sciencemag.org/ on September 11, 2020